Virology 523 (2018) 129–139

Contents lists available at ScienceDirect

Virology

journal homepage: www.elsevier.com/locate/virology

A quantitative assessment of dynamical differences of RSV infections in vitro and in vivo

Gilberto González-Parra[a], Hana M. Dobrovolny[b,*]

[a] Department of Mathematics, New Mexico Tech, Socorro, NM, United States
[b] Department of Physics and Astronomy, Texas Christian University, Fort Worth, TX, United States

ARTICLE INFO

Keywords:
Respiratory syncytial virus
Fusion inhibitor
Pediatric
Elderly
Mathematical model
African green monkey

ABSTRACT

Experimental results in vitro and in animal models are used to guide researchers in testing vaccines or treatment in humans. However, viral kinetics are different in vitro, in animals, and in humans, so it is sometimes difficult to translate results from one system to another. In this study, we use a mathematical model to fit experimental data from multiple cycle respiratory syncytial virus (RSV) infections in vitro, in african green monkey (AGM), and in humans in order to quantitatively compare viral kinetics in the different systems. We find that there are differences in viral clearance rate, productively infectious cell lifespan, and eclipse phase duration between in vitro and in vivo systems and among different in vivo systems. We show that these differences in viral kinetics lead to different estimates of drug effectiveness of fusion inhibitors in vitro and in AGM than in humans.

1. Introduction

Infants and the elderly are most likely to experience serious illness or death from respiratory syncytial virus (RSV) (Borchers et al., 2013). To alleviate this burden, researchers have long been searching for an antiviral or vaccine that would effectively treat or prevent RSV (Collins and Melero, 2011; Esposito and Pietro, 2016). Several fusion inhibitors have been tested in vitro and in animal models (Zheng et al., 2016; Perron et al., 2016; Bonfanti et al., 2008; Feng et al., 2015; Bond et al., 2015; Lundin et al., 2010; Andries et al., 2003; Cianci et al., 2005), but some have had difficulty making the transition from animals to humans. Likewise, many RSV vaccines have been tested in animal models, with the induced antibody neutralizing ability tested in vitro, but promising candidates have not been as effective in humans (Esposito and Pietro, 2016).

For RSV, as for many viral infections, in vitro and animal models are the primary systems of study used to understand the dynamics of the infection (Weiss et al., 2014). These same systems are also the primary test beds for new antivirals and vaccines. It is not clear, however, how experimental results translate from one system to another (Bem et al., 2011). This is particularly important when trying to extrapolate antiviral or vaccine studies from in vitro or animal models to humans (Jorquera et al., 2016). Differences in cell tropism (Jia et al., 2014; Taylor, 2017; Shakeri et al., 2015), the immune response (Taylor, 2017; Jorquera et al., 2016; Sacco et al., 2015), and other physiological interactions (Zanin et al., 2016) between these systems might lead to differences in infection dynamics and the efficacy of treatment. Our lack of understanding of how differences in preclinical systems and humans alter disease dynamics leads to a paltry ~ 12% success rate in moving treatments from preclinical through Phase III testing and an ~ 11% success rate for vaccines to move through the development pipeline (Davis et al., 2011).

In addition to differences between experimental systems and humans, there are also differences in infection dynamics in individual humans. Broadly, there are differences in the immune response to RSV between healthy adults, children, and the elderly (Walsh et al., 2013; Mcintosh et al., 1978; Chung et al., 2007). This leads to more serious infections, with higher mortality and hospitalization, in children and the elderly as compared to healthy adults (Borchers et al., 2013; Stein et al.,; Anderson et al., 2016). This also leads to differences in clinical manifestation of the disease with children and the elderly exhibiting more severe symptoms and showing a greater propensity for involvement of the lower respiratory tract (Dayar and Kocabas, 2016; Shi et al., 2015; Park et al., 2016).

While there are differences in host-cell interactions when RSV is introduced into different hosts, viral replication follows a similar basic process in all hosts. Respiratory syncytial virus is an enveloped virus containing negative-sense RNA that has 10 genes encoding 11 proteins (Lee et al., 2012). RSV binds to host cells through the G transmembrane protein (Teng et al., 2001) and fuses via the F transmembrane protein

* Corresponding author.
E-mail address: h.dobrovolny@tcu.edu (H.M. Dobrovolny).

https://doi.org/10.1016/j.virol.2018.07.027
Received 22 April 2018; Received in revised form 24 July 2018; Accepted 25 July 2018

(Feldman et al., 2000). The F protein is also responsible for fusing membranes of neighboring cells giving rise to the syncytia that give the virus its name (Gonzalez-Reyes et al., 2001). Once internalized, the genome is released into the cell's cytoplasm where transcription and replication take place (Follett et al., 1975). Newly formed genomes and proteins migrate to the surface of the cell where they form filamentous viral particles before breaking through the cell membrane (Vanover et al., 2017; Shaikh et al., 2012). The final stages of filament maturation and budding of the virus from the cell are mediated by the matrix M protein (Shahriari et al., 2016; Foerster et al., 2015). These basic steps of replication can be captured and reproduced using mathematical equations to help us improve our understanding of RSV dynamics.

Mathematical models of the in-host dynamics of viral infections have been used to quantitatively describe the infection process for many different viral infections (Baccam et al., 2006; Nguyen et al., 2015; Perelson et al., 1996; Neumann et al., 1998; González-Parra and Dobrovolny, 2015; González-Parra et al.,). Specifically, mathematical models are now being used to quantitatively compare infections caused by different strains of virus (Pinilla et al., 2012; Paradis et al., 2015; Simon et al., 2016; Petrie et al., 2015) or by different infections (González-Parra et al., 2018). The simplest mathematical model captures the basic steps of virus entry, internal replication, and viral budding (Perelson et al., 1996; Baccam et al., 2006) and can be used to simulate a variety of scenarios including single-cycle infection and multiple-cycle infection by changing the initial conditions (Pinilla et al., 2012; Paradis et al., 2015; Beggs and Dobrovolny, 2015), or in vivo infections by changing the values of model parameters to reflect the effect of the immune response. Such studies lead to an understanding of which parts of the viral replication cycle are changed when moving from one virus-host system to another.

In this paper, we use a viral kinetics model to estimate parameters for RSV infection in five different systems: in vitro, African green monkey (AGM), elderly patients, pediatric patients, and healthy adults. This allows us to quantitatively compare the viral replication cycle in these different systems. We find differences in several viral kinetics parameters between the groups, including the viral clearance rate, the cell's productively infectious lifespan, and the duration of the eclipse phase. We show that these differences alter the effectiveness of drug treatment in the different systems such that EC_{50} measured in vitro or in animals does not reflect the EC_{50} needed for treatment of humans.

2. Material and methods

2.1. Models

We use two mathematical descriptions of viral dynamics. The first is an empirical description of the viral time course, first presented by Holder and Beauchemin (2011). While this model does not give insight into the underlying dynamics of the infection, it allows measurement of some of the important viral titer curve characteristics (González-Parra et al., 2016). The model is given by the equation

$$V(t) = \frac{2V_p}{\exp[-\lambda_g(t-t_p)] + \exp[\lambda_d(t-t_p)]}, \tag{1}$$

where λ_g and λ_d are the exponential growth and decay rates, respectively, V_p is the peak viral titer, and t_p is the time of viral titer peak. While this equation will not reproduce a single-cycle experiment well since the viral growth in this case is not exponential (Holder and Beauchemin, 2011), it can be used for multiple-cycle experiments where viral growth is exponential (González-Parra et al., 2016). The in vitro data used in this study were all from experiments with an MOI of less than 1 (González-Parra et al., 2018) with the exception of the data from Liesman et al. (2014), which has an MOI of 1. Note that this equation does not fully capture all the dynamics of a viral infection, as it notable neglects any initial transient changes in viral load, so is not meant to fully characterize viral kinetics, but it does estimate features that are traditionally used to characterize infections (González-Parra et al., 2016). This simple equation has only four independent parameters, making parameter estimation simpler than for a more complex, kinetic model of viral infection. We require at least four experimental data points, with at least two during the growth phase and two during the decay phase, to identify the parameters (González-Parra et al., 2016).

Our second model is a viral kinetics model that incorporates the basic biological processes that occur during the infection. The model is an extension of the basic viral infection model for influenza described in Baccam et al. (2006),

$$\begin{aligned}
\frac{dT}{dt} &= -\frac{\beta}{N}TV \\
\frac{dE_1}{dt} &= \frac{\beta}{N}TV - \frac{n_E}{\tau_E}E_1 \\
\frac{dE_j}{dt} &= \frac{n_E}{\tau_E}E_{j-1} - \frac{n_E}{\tau_E}E_j \quad \text{for } j = (2,\ldots,n_E) \\
\frac{dI_1}{dt} &= \frac{n_E}{\tau_E}E_{n_E} - \frac{n_I}{\tau_I}I_1 \\
\frac{dI_j}{dt} &= \frac{n_I}{\tau_I}I_{j-1} - \frac{n_I}{\tau_I}I_j \quad \text{for } j = (2,\ldots,n_I) \\
\frac{dV}{dt} &= p\sum_{j=1}^{n_I} I_j - cV.
\end{aligned} \tag{2}$$

In the model, virus V, infects target cells, T, at rate β. Once infected, the cells enter an eclipse state, E, during which they are producing viral proteins and RNA, but not yet releasing virus. After an average time τ_E, the cells transition to a productively infectious state, I, where they are producing virus at rate p. After an average time τ_I, the productively infectious cells die. Virus loses infectivity at a rate c.

This model captures the basic processes of viral entry, replication within the cell, and release of new virions, so can be applied to both in vitro and in vivo systems (Pinilla et al., 2012; Paradis et al., 2015; González-Parra and Dobrovolny, 2015; Petrie et al., 2015). While our model will be applied to patient data, we do not include an explicit immune response since there is not enough data to accurately determine the values of the extra parameters needed to describe the immune response. Instead, our estimates of the parameters in these different systems will reflect the effect of the immune response. For example, we expect the value of c, the viral clearance rate, to be larger in vivo than in vitro since in vivo systems include an antibody response that helps clear virus from the system.

This model assumes a gamma distribution, represented by the multiple compartments for E and I, for the transition times between the eclipse state and the productively infectious state, as well as for the transition times between the productively infectious and dead cells. The number of compartments in the eclipse state is given by n_E while the number of compartments in the productively infectious state is given by n_I. Models that include non-exponential transitions between cell states more accurately reproduce experimental viral kinetics (Holder and Beauchemin, 2011). This model has more parameters than the empirical model, some of which cannot be identified with viral titer data alone (Miao et al., 2011; Pinilla et al., 2012).

2.2. Experimental data

Our aim in this study is to compare the dynamics of RSV in several different experimental and clinical systems, thus we combined data from several different sources, summarized in Table 1 and briefly described below.

- Experimental data from in vitro RSV infections was collected from the literature as described in González-Parra et al. (2018). While we required that all in vitro data use the same strain of RSV (A2), the cell culture and experimental procedures for each data set varied since they were drawn from multiple sources. The sources and some details of the data sets are included in Table 2.

Table 1
Summary of the different experimental data sets used in this study.

System	Source	Number of Data Sets
in vitro	literature (González-Parra et al., 2016)	8
AGM	Ispas et al. (2015)	9
Elderly	Walsh et al. (2013)	27
Pediatric	data provided by Janssen R&D	13
Healthy adults	Lee et al. (2004)	8

Table 2
Summary of literature sources for in vitro data.

Paper	Figure*	Cell type
Bermingham and Collins (1999)	4B	HEp-2
Brock et al. (2003)	1B	HEp-2
Liesman et al. (2014)	1C	HAE
Marquez and Hsiung (1967)	2	HEp-2
Shahrabadi and Lee (1988)	2A	HEp-2
Straub et al. (2011)	2A	A549
Villenave et al. (2011)	4A (A2 strain)	PBEC
Villenave et al. (2012)	1A (A2 strain)	WD-PBEC

* Refers to the figure numbers in the original paper.

- Experimental data from RSV infections in African green monkeys (AGM) comes from the control animals in the two TMC353121 treatment studies described in Ispas et al. (2015). In this study, AGM were infected with RSV A2 and bronchoalveolar lavage fluid (BALF) was collected every 2 days.
- We also used data from a study of elderly patients infected with RSV (Walsh et al., 2013). These patients presented with influenza-like symptoms at the hospital and were tested for RSV. Viral titer measurements were taken on the day patients presented with symptoms and for several days after. Viral titer measurements were taken from nasal swab specimen. Since this was not a challenge study, we do not know the initial time of infection of the patients, but will use the time of symptom onset as an estimate for the time of infection. Several RSV challenge studies have indicated that symptom scores increase slightly as soon as 1 dpi (DeVincenzo et al., 2015, 2010, 2010; Lee et al., 2004; DeVincenzo et al., 20152015), making this a reasonable proxy.
- A second prospective study in pediatric patients, with data provided by Janssen R&D Belgium, is also used in this study. As before, RSV was diagnosed upon presentation at a doctor or hospital with viral titer measurements taken daily via nasal swabs from that point onwards. Here again, we do not know the actual time of infection. We use time of symptom onset as an initial estimate of the time of infection, but for some patients this resulted in an unrealistically high viral titer growth rate. In these cases, we required that the time of infection be such that the estimated viral titer at $t = 0$ be below the threshold of detection.
- Data for RSV infections in adults was taken from a challenge study by Lee et al. (2004). In this study, healthy adults were inoculated with the A2 strain of RSV and viral titer was sampled daily via nasal washes for 12 days.

For all experimental data, we limited our study to patients who had at least four viral titer measurements above the threshold of detection to ensure parameter identifiability for at least the empirical model.

2.3. Fitting algorithms

The model was fit to each data set in order to obtain estimates for the parameter values. We determined the best fit by minimizing the sum of squared residuals (SSR),

$$\mathrm{SSR} = \sum_{i=1}^{n} (y_i - f(t_i; \theta))^2, \tag{3}$$

where n is the number of experimental data points, y_i are the values of the experimental data points, $f(t_i; \theta)$ are the model predictions at the times when experimental data were measured, and θ is the set of parameters to be estimated. A small SSR indicates a tight fit of the model to the experimental data.

We used two algorithms to find the minimum SSR. We initially used a genetic algorithm (Golberg, 1989) which performs a very broad search of the parameter space and is less dependent on the initial guess. Over many iterations, the population of parameter estimates "evolves" toward an optimal solution (Golberg, 1989; Holland, 1992; Conn et al., 1997). We ran the global optimization algorithm 200 times with different scenarios (initial guess, parameters of the optimization process) in order to improve the probability of finding the global optimum parameter set. Once the genetic algorithm found a good fit, these parameters were used as the initial guess for the trust-region-reflective and interior point algorithms (Coleman and Li, 1996; Press et al., 1992), which search a more localized region of the parameter space. The use of several different algorithms increases the probability of finding the global minimum for the SSR. All fitting was implemented in Matlab using the `ga` and the `fmincon` functions of the `optimization` package. Note that we do not calculate error or confidence intervals for individual parameter estimates since we are aggregating parameter estimates into groups and can use animal-to-animal differences as an indicator of the variability in parameter values.

For the empirical model, no constraints were used in the fitting process. For the viral kinetics model, we assume that all infections are multiple-cycle (low MOI) infections. The MOI for in vitro data used here is 1 or less (González-Parra et al., 2018). For healthy adult data, we estimate MOIs of 9×10^{-6} and 9×10^{-5} for the low and high doses, based on the inocula of $10^{3.7}\mathrm{TCID}_{50}$ and $10^{4.7}\mathrm{TCID}_{50}$ (Lee et al., 2004) and the estimated number of epithelial cells in the human respiratory tract (4×10^{8} Baccam et al., 2006). Similarly, for AGM, we estimate an MOI of 2.5×10^{-5}. We can also roughly estimate a possible MOI for the pediatric and elderly patients assuming that the primary mode of RSV transmission is aerosolized particles (Kulkarni et al., 2016). Measurements of RSV in the air near a pediatric patient found, on average, 10^{6} pfu 1 m from the patient and $10^{5.6}$ pfu 5 m from the patient (Kulkarni et al., 2016), so the MOIs in this case are 0.0025 at 1 m and 0.001 at 5 m. To reproduce a multiple cycle infection in our model, we fixed the initial number of target cells to $T_0 = 1$ and assumed that the infection was started with an unknown (to be fitted) initial viral inoculum, assuming that there are initially no cells in any of the eclipse or productively infectious compartments. We know that some parameters are not identifiable for this model (Miao et al., 2011; Pinilla et al., 2012), so we fixed the number of compartments in both the eclipse and productively infectious phases, $n_I = n_E = 60$, and set bounds on the searched parameter space as follows: $10^{-1} - 10^{16}$/d for p; $10^{-14} - 100$/d for β; 10^{-5}–1000/d for c; $10^{-5} - 1000$/d for τ_I and τ_E; $10^{-12} - 10^{4}$ for V_0. Note that the bounds are quite large and are meant to eliminate the possibility of finding biologically unrealistic parameter values.

It is difficult to compare parameter estimates from different experiments since the units of viral titer depend on the assay used to determine the viral titer. For example, the viral count from plaque assays is ~ 0.7 the viral count from endpoint dilution assays, but this is only an approximate relationship based on statistical calculations and will not hold for all experiments (Mistry et al., 2018). More fundamentally, even using the same assay and same techniques, viral quantification has problems with reproducibility (Paradis et al., 2015). Since viral titer units vary from one experiment to the next, comparison of parameters such as p and β is meaningless. Therefore, we focused on parameters which have a universal standardized unit. In addition to the mean duration of the eclipse phase τ_E and the mean duration of the productively infectious phase τ_I, the infecting time, $t_{\mathrm{inf}} = \sqrt{2/p\beta}$, Holder

and Beauchemin (2011), which is the average time between release of a virion from a productively infectious cell and infection of another cell, was calculated.

2.4. Simulation of fusion inhibitor treatment

We simulate treatment with a fusion inhibitor, the most common type of RSV antiviral (Sun et al., 2013), by multiplying the infection rate by $(1-\varepsilon)$, where ε is the drug efficacy and ranges from 0 (no effect) to 1 (complete inhibition). The efficacy is related to the drug concentration through the E_{max} model (Holford and Sheiner, 1981),

$$\varepsilon(t) = \varepsilon_{\max}\frac{C(t)}{C(t)+IC_{50}} \tag{4}$$

where $C(t)$ is the drug concentration, $\varepsilon_{\max}$ is the maximum efficacy of the drug such that $0 < \varepsilon_{\max} \leq 1$, and IC_{50} is the concentration of drug necessary to inhibit the response by 50%. We assume that the maximum efficacy of the drug is 1, and we express drug concentration in units relative to the IC_{50}, so that we can set $IC_{50} = 1$ without loss of generality.

3. Results

3.1. Data sets

The data sets are shown, in groups, in Fig. 1. The in vitro, AGM, and particularly the pediatric data sets reach higher viral loads than the human adult groups. The in vitro data sets appear to have a more gradual rise and decline than the other data sets. For the remaining data sets (AGM, pediatric, elderly, healthy adult), each line represents measurements from a single individual, which gives a better indication of the actual growth and decay rates of the virus in these systems. The data for elderly patients consists mostly of the viral decay phase of the infection. Since this data is from a prospective study, we do not know the time of infection (we have set time of symptom onset as $t = 0$), so the individual viral time courses do not align very well, making it difficult to discern the general trend of the viral time course.

3.2. Empirical model

Fits of the empirical model produce parameter estimates that describe the time course of viral burden, but don't provide much insight into viral kinetics. Figures showing the experimental data and model fits to the data are included in the supplementary material. Median values of parameter estimates for each data set are presented in Table 3 with estimates for each individual viral time course included in the supplementary material. The results are summarized in Fig. 2.

The viral growth rate appears to be about the same in all systems (Fig. 2(a)). There is much more variability in the growth rate estimates for elderly and pediatric data sets (both prospective studies) where viral titer measurements during the growth phase were limited, leading to less reliable estimates of the growth rate in these systems. The viral decay rate is highest in AGM and healthy adults and lowest in vitro (Fig. 2(b)). Time of viral peak is lower in vitro than in the other systems (Fig. 2(c)). There is again more variability in the time of viral peak estimates for the elderly and pediatric patients than in the other systems largely because we are estimating the time of infection for these data.

3.3. Viral kinetics model

Next, data from the same set of studies were analyzed using the viral kinetics model to obtain some insight into the processes governing the viral life cycle. With this analysis, we estimated t_{inf}, the infecting time; c, the clearance rate; τ_I, the infectious lifespan; and τ_E, the duration of the eclipse phase. Median values for all data sets are given in Table 4 with fits and parameter estimates for individual viral time courses included in the supplementary material. The results are summarized in Fig. 3.

The infecting time is highest in vitro and lowest in pediatric and healthy adult groups (Fig. 3(a)). The productively infectious lifespan is longest in elderly and healthy adults, and is markedly shorter in the remaining three groups (Fig. 3(b)). The eclipse duration is longest in elderly and healthy adults, and markedly shorter in the remaining three groups (Fig. 3(c)). Finally, the viral clearance rate shows a trend similar to the viral decay rate of the empirical model, with AGM and healthy adults having the highest clearance rates and in vitro systems having the lowest (Fig. 3(d)).

To give an overview of typical infections in these different systems, we used the viral kinetics model with median estimated parameter values for each group to simulate a typical infection for each group (Fig. 4). There are some clear differences in the viral dynamics of RSV in these different groups. The pediatric group sheds much more virus than any other system. We can also clearly see the slower viral decay of the in vitro system compared to the other systems. The healthy adults and elderly show similar time courses although they are different from the AGM and in vitro systems often used for testing treatments in humans. Note that we have initiated each infection with the initial viral inoculum found through fitting. If the same initial viral inoculum is assumed for all infections, we will see a shift in the time of peak of the infections. The viral growth rate and peak viral titer are not changed by changes in initial inoculum, so the time of peak is shifted because there is initially more (or less) virus and the infection starts closer (or further) to the peak it will reach.

3.4. Application of a fusion inhibitor

In vitro and animal model systems are used not only to study the course of an infection, but are also used to test new treatments. In order to effectively use the results of in vitro and animal treatment studies, we need to understand how the effect of treatment might change as we move from one system to another. We simulate prophylactic treatment with a fusion inhibitor using viral titer at 48 hpi as the endpoint measurement. Fig. 5 shows the predicted reduction in viral titer at 48 hpi for treatment with a fusion inhibitor in the systems included in this study. This curve allows measurement of the EC_{50}, which is the drug concentration needed to reduce viral titer at 48 hpi by 50%, and is a measure of the effectiveness of an antiviral. We find that the in vitro and AGM systems underestimate the EC_{50} for the healthy adults and elderly patients, although they more closely reflect the EC_{50} for pediatric patients. We also simulate the more realistic scenario of fusion inhibitor treatment initiated at 48 hpi. Here, the endpoint measurement is reduction in viral titer 48 hpi after initiation of treatment. We see even more drastic differences in the predicted outcomes for different systems. In vitro, there are some drug concentrations that lead to an increase in the viral load, an effect not seen in other systems. This is a result of measuring effect of the drug at a fixed time. Fusion inhibitors reduce both the peak viral load and the growth rate of the infection (Beggs and Dobrovolny, 2015; González-Parra and Dobrovolny, 2018). Since the growth rate is reduced, treated infections reach their peak viral load later than untreated infections. Thus if the measurement time occurs after the peak of an untreated infection, the viral load might be lower for the untreated infection, since it is decreasing from its peak value, than for a treated infection, which might still be increasing towards its peak value. Since the in vitro infection peaks before the measurement time, we see this seemingly contradictory effect only in this system. More strikingly, our models predict that fusion treatment at 48 hpi will have no effect on infections in healthy adults and the elderly.

4. Discussion

While there are known differences in immune response and virus-

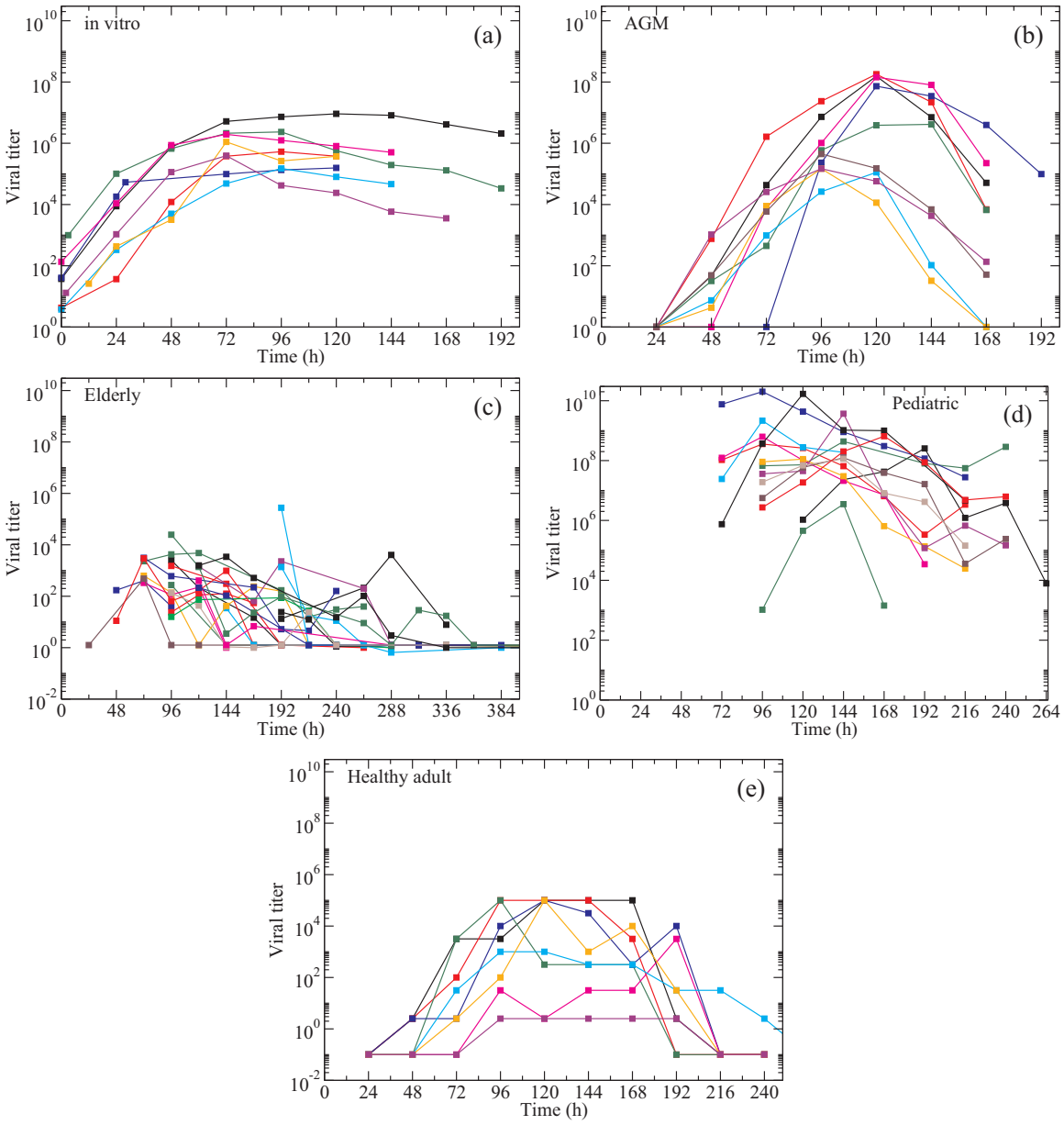

Fig. 1. Study data. Experimental data from (a) in vitro RSV infections, (b) infections in african green monkeys, (c) elderly adults (d) pediatric patients, and (e) healthy adults. Note that time of infection onset is not known for elderly and pediatric data but is estimated as described in Methods.

Table 3
Median estimated parameter values for the empirical model (Eq. (1)).

Data	λ_g (/h)	λ_d (/h)	t_p (h)
in vitro	0.17	0.023	58.7
AGM	0.21	0.19	114
Elderly	0.060	0.038	139
Pediatric	0.086	0.086	128
Healthy adult	0.14	0.13	130

host interactions between in vitro systems, animal models, and humans (Jia et al., 2014; Taylor, 2017; Shakeri et al., 2015; Jorquera et al., 2016; Sacco et al., 2015; Zanin et al., 2016), this is the first study to quantify the effects of these differences on the time course of a viral infection. Our analysis showed that viral decay rate and viral clearance rate are higher in systems where there is a strong immune response (AGM, healthy adults) and low in systems with limited immune response (in vitro). These parameters most likely reflect the action of antibodies which bind to virus, inactivating the virus (Sarmiento et al., 2007), or neutrophils and macrophages, which can also remove circulating virus (Yui et al., 2003; Russell et al., 2017), but they could also be influenced by the action of cytotoxic T lymphocytes which kill infected cells and therefore lower the overall amount of virus produced (Rutigliano et al., 2004). We also found that the productively infectious lifespan in adult and elderly infections tends to be longer than either in vitro or AGM infections. A possible mechanism for this difference is the finding that the RSV fusion protein activates p53 which then causes apoptosis in HEp-2 and A549 cells (Eckardt-Michel et al., 2008), common in vitro cell lines for RSV infection. However, in human tracheobronchial epithelial cells, RSV was shown to decrease p53, prolonging the lifespan of productively infectious cells (Groskreutz et al., 2007). Our study also found other differences, longer eclipse phases in elderly and healthy adults, and an earlier time of peak for in vitro systems, although the possible mechanisms for these differences are not clear and will need further investigation.

One of the important applications of in vitro and animal model

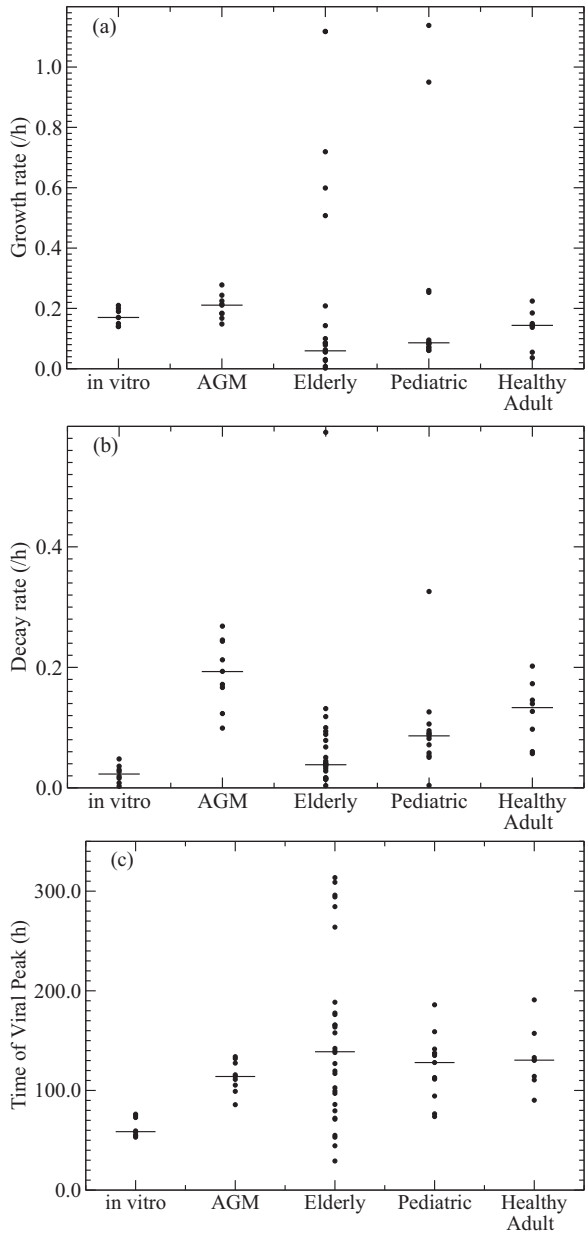

Fig. 2. Comparison of empirical model parameters. Graphs show the distributions of (a) growth rate, (b) decay rate, (c) time to peak viral titer estimated from fits of the empirical model for RSV in different systems. Median values are indicated with a solid black line.

Table 4
Median estimated parameter values for the viral kinetics model (Eq. (2)).

Data	t_{inf} (h)	c (/h)	τ_I (h)	τ_E (h)
in vitro	3.3	0.030	11.8	6.38
AGM	1.9	0.35	8.64	7.44
Elderly	1.9	0.13	47.7	58.3
Pediatric	1.2	0.065	24.2	7.01
Healthy adult	0.95	0.32	46.3	62.8

systems is the development and testing of antivirals. While pediatric and elderly patients are the primary targets for new antivirals, clinical studies in these groups are risky and so in vitro, animal, and healthy adults are used for preliminary studies. Unfortunately, there are known limitations of these systems. In particular, AGM are only semi-permissive to RSV (Taylor, 2017; Kakuk et al., 1993), showing few clinical symptoms and limited histopathological changes (Jones et al., 2012; Ispas et al., 2015). Healthy adults also have mild disease as compared to elderly or pediatric patients (Hall et al., 2001; Houben et al., 2010; Falsey and Walsh, 2005), with most healthy adults having only mild respiratory symptoms (Hall et al., 2001; Lee et al., 2004; Bagga et al., 2013; Mills et al., 1971), lower viral loads (Lee et al., 2004; Bagga et al., 2013) and only occasional involvement of the lower respiratory tract (Hall et al., 2001). This is thought to be due to the protective effect of immunity from previous RSV infections which results in shorter duration of infection and lower viral load (Hall et al., 1991; Lee et al., 2004; Mills et al., 1971). A key difference between infections in healthy adults and those in pediatric or elderly patients is the immune response (Malloy et al., 2013). Both pediatric and elderly patients have a diminished immune response, due to an immature immune system in infants (Ruckwardt et al., 2016; Tregoning and Schwarze, 2010) or immune senescence in the elderly (Walsh et al., 2013), as compared to healthy adults. This leads to more severe infections (Openshaw et al., 2017; Mosquera et al., 2014), often spreading into the lower respiratory tract (Naorat et al., 2013; Kaneko et al., 2001; Shi et al., 2015; Atwell et al., 2016).

These differences in disease dynamics are expected to result in different responses to antivirals. We simulated the impact of differences in the systems on prophylactic use of fusion inhibitors using our parameter estimates and found that the in vitro and animal models underestimated the EC_{50} needed to treat healthy adults and elderly. In vitro and animal derived EC_{50} estimates are used as a guide when testing new antivirals in humans, so this could result in use of too low a dose in humans during initial testing, giving the impression that the antiviral is ineffective in humans. We also see that pediatric patients need less drug to reduce their viral load than most other groups in this study. Note that we express drug concentrations relative to IC_{50}, so we already take into account the smaller doses needed due to the smaller body mass of children (Mulugeta et al., 2016; Dunne et al., 2011). Our study indicates that drug doses in children need further reduction due to differences in infection dynamics between adults and children. Our models predict even more striking differences when fusion inihibitor treatment is initiated after the onset of infection. In this case, models predict that despite being effective in vitro and in AGM, fusion inhibitors show little effect in healthy and elderly adults. Changes in the efficacy of a drug when moving from in vitro to in vivo systems have been previously noted for HIV antiretrovirals (Fang and Jadhav, 2012), where measured values of EC_{50} were as much as 9 times higher in vivo than in vitro. While new types of in vitro assays have been proposed with the hope that they will provide more consistent EC_{50} measurements (Beggs and Dobrovolny, 2015; Ferguson et al., 2001), they have not yet been tested.

Our study is limited by the type of data available. Our in vitro data was inconsistent since each data set came from a different lab where experimental procedures might be slightly different. Most of these infections also took place in different types of cells, introducing variability in the estimated parameters. The more gradual rise and decay of the in vitro data might be the effect of averaging measurements from several in vitro infections, since averaging tends to smooth out abrupt increases or decreases. Additionally, the elderly and pediatric data were from prospective studies, so the time of infection of individual patients was not known, introducing a time shift which could potentially be reflected in some of the parameter estimates. The data in these studies also often does not include the full viral growth phase since the first viral load measurement is taken some time after the patient experiences symptoms. Pediatric and elderly patient data might also be biased towards more severely ill patients since only patients who presented at a hospital were included in the studies, patients with mild illness are not represented in this data. This could affect estimates of some parameters as viral load is correlated to clinical symptoms (DeVincenzo et al., 2010; Buckingham et al., 2000). Additionally, nasal secretion specimen were collected using different methods in AGM, pediatric/elderly, and

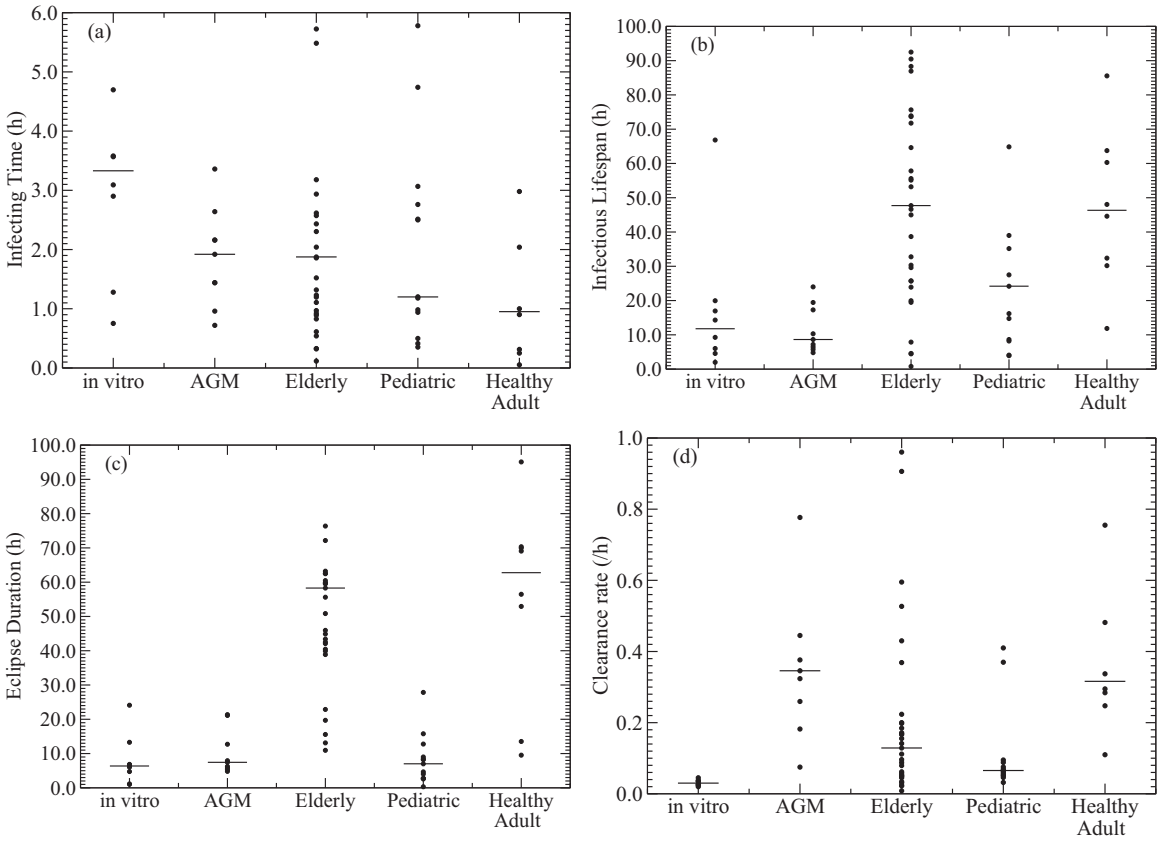

Fig. 3. Comparison of viral kinetics parameters. Graphs show the distributions of (a) infecting time (t_{inf}), (b) duration of the productively infectious phase (τ_I), (c) duration of the eclipse phase (τ_E), and (d) clearance rate (c) estimated from fits of the gamma model for RSV in different systems. Median values are indicated with a solid black line.

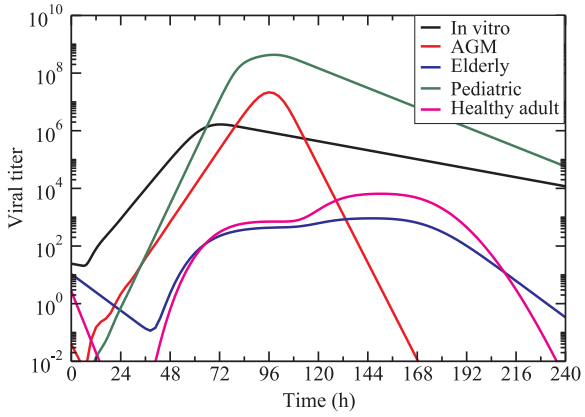

Fig. 4. Simulated viral titer time courses. Predicted time courses of RSV in different systems using the median values (Table 4) for each of the parameters in the viral kinetics model (Eq. (2)). Note that elderly and pediatric patient parameters are based on data with estimated time of infection onset.

in healthy adults. While no study exists comparing viral detection in BALF (used for AGM) to either nasal swabs or washes, one study compared bacterial detection in BALF and nasopharyngeal swab (NPS), finding that BALF was more sensitive in detecting the virus (Capik et al., 2017). Several comparisons of nasopharyngeal aspirates (NPA) and nasal swab have concluded that the nasal aspirate more readily allows for detection of virus (Blaschke et al., 2011; Meerhoff et al., 2010). If we can assume that both collection methods affect the results in the same way for every patient, this amounts to an upward or downward shift in the data. Since the relative shape of the curve will not change by vertical shifting, we do not believe that this will have a significant effect on the parameters values. Finally, differences in sampling times and sampling techniques could affect the parameter estimates. For an ideal comparison of different experimental systems, we would need in vitro, pre-clinical, and challenge study data with viral loads measured in a consistent manner. We would additionally require that in each system, full viral time courses are measured so that both the full viral growth phase and the full viral decay phase are captured.

This kind of consistent and complete data might allow for a more detailed analysis than described here. For example, our model does not explicitly include an immune response. While the effect of the immune response is captured in the estimated values of the parameters in the current model, explicitly including the immune response in the model would allow us to compare immune parameters across the different systems, particularly if some measurements of the immune response were included in the study. Time course measurements of the same immune components in each of these systems will allow us to separate out variability in kinetics due to immune responses from variability due to other host-pathogen interactions. More detailed data might also allow comparison of structurally different models for the different systems. Here, we used the same model for all the different groups, but it's possible that these different systems are not necessarily described by the same equations. For example, if we extended the model to include an immune response, it would not make sense to include equations for antibodies and cytotoxic lymphocytes in the model for an in vitro system, but these equations should be included for the remaining systems.

Another possible confounder in the data is the fact that the pediatric and elderly data was not separated by strain or subtype, which could cause variation in viral kinetics. In terms of clinical severity, some studies have found that RSV A causes more severe illness than RSV B (Rodriguez-Fernandez et al., 2018; Papadopoulos et al., 2004; Hall

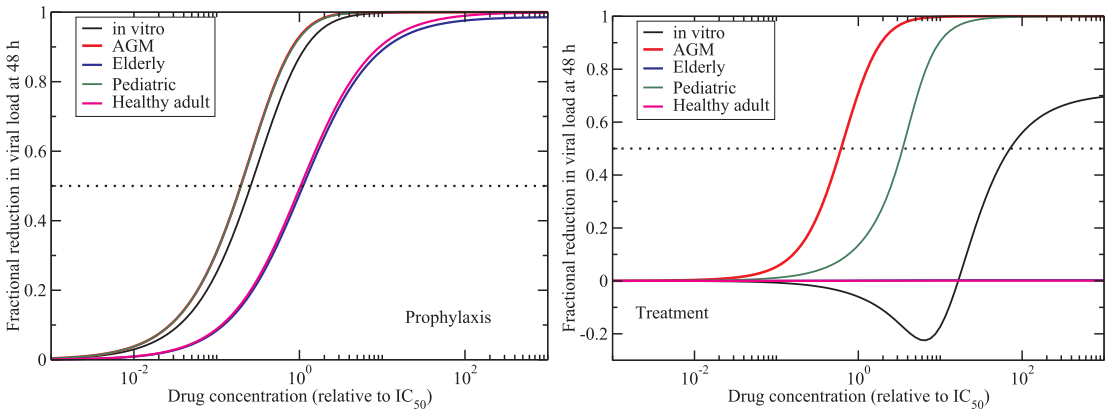

	in vitro	AGM	Elderly	Pediatric	Healthy Adult
EC_{50} (prophylactic)	0.27	0.20	1.0	0.20	1.0
EC_{50} (treatment)	73	0.63	–	3.6	–

Fig. 5. Simulated fusion inhibitor treatment. (left) Predicted reduction in viral titer at 48 hpi as a function of fusion inhibitor concentration in different systems for RSV prophylaxis. (right) Predicted reduction in viral titer at 96 hpi as a function of fusion inhibitor concentration in different systems for treatment initiated at 48 hpi. We use the median values (Table 4) for each of the parameters in the viral kinetics model (Eq. (2)). The dashed line indicates a 50% reduction.

et al., 1990; Jafri et al., 2013; Nguyen et al., 2013; Gilca et al., 2006). Others contradict this, finding either the reverse (Hornsleth et al., 1998) or no statistically significant difference between severity of RSV A and RSV B infections (DeVincenzo, 2004; Hendry et al., 1986; McIntosh et al., 1993; Russi et al., 1989). Kinetically, there appear to be no significant differences in viral load (DeVincenzo, 2004) between the two RSV subtypes, although some studies have noted differences in viral load between specific strains of RSV A (Lukacs et al., 2006; Stokes et al., 2011). Most notably, some researchers have found differences in the immune responses to RSV A and RSV B, including differences in neutrophils (Rodriguez-Fernandez et al., 2018) and cytokines (Levitz et al., 2012), while another study noted no significant difference in cytokine response (Bermejo-Martin et al., 2008). Within a particular subtype, differences between immune responses to strains of RSV B (Levitz et al., 2017, 2012) and strains of RSV A (Stokes et al., 2011; Lukacs et al., 2006) have also been observed. With such mixed results, it is difficult to assess whether the inclusion of different strains of RSV in the elderly and pediatric data had a significant impact on our results.

Our model also does not account for the formation of syncytia. While it is clear that they can alter RSV viral transmission dynamics in some cell lines (Shigeta et al., 1968), there does not seem to be enough information available about the behavior of RSV syncytia to correctly incorporate them into the model. For example, there is evidence from HIV that syncytia formed by HIV can continue to produce virus (Symeonides et al., 2015, Sylwester et al., 1997; Chowdhury et al., 1992). If that is also the case for RSV syncytia, then we need to know whether viral production rates for multinucleated cells are greater than, less than, or comparable to mononuclear cells. We also need to know how long multinucleated cells live as compared to mononuclear cells and whether the lifespan or production rates depend on size as seems to be the case for HIV-induced syncytia (Sylwester et al., 1997). A further consideration is which cells are involved in syncytia formation. Can only cells in the eclipse and productively infectious phases fuse, since they have the F-protein on their surfaces, or can one of these cells fuse with a target cell that will not yet have the F protein? While there have been some detailed studies of the formation, lifespan and viral production of HIV-induced syncytia (Symeonides et al., 2015, Sylwester et al., 1997; Chowdhury et al., 1992), there do not appear to be similar studies for RSV-induced syncytia. Such studies will be needed to help guide development of mathematical models that incorporate the effect of syncytia. Since syncytia are not explicitly included in the model used here, their effect is implicitly included in the estimated values of model parameters.

Nonetheless, our study quantified differences in the viral replication cycle between in vitro, animal, and human infections and showed that these differences could lead to differences in the estimated efficacy of antivirals.

Acknowledgements

Elderly patient data was provided by Dr. Ann Falsey and Dr. Ed Walsh of University of Rochester. Pediatric patient data was provided by Janssen R&D Belgium. The authors would like to acknowledge the assistance and helpful advice provided by Gabriela Ispas, Filip De Ridder, Dymphy Huntjens, and Dirk Roymans of Janssen R&D Belgium. Hana M. Dobrovolny received funding from Janssen R&D Belgium (610765), and Gilberto Gonzalez-Parra's salary was paid by a grant from Janssen R&D Belgium.

Appendix A. Supplementary data

Supplementary data associated with this article can be found in the online version at doi:10.1016/j.virol.2018.07.027.

References

Anderson, N.W., Binnicker, M.J., Harris, D.M., Chirila, R.M., Brumble, L., Mandrekar, J., Hata, D.J., 2016. Morbidity and mortality among patients with respiratory syncytial virus infection: a 2-year retrospective review. Diagn. Microbiol Infect. Dis. 85 (3), 367–371. https://doi.org/10.1016/j.diagmicrobio.2016.02.025.

Andries, K., Moeremans, M., Gevers, T., Willebrords, R., Sommen, C., Lacrampe, J., Janssens, F., Wyde, P., 2003. Substituted benzimidazoles with nanomolar activity against respiratory syncytial virus. Antivir. Res. 60 (3), 209–219. https://doi.org/10.1016/j.antiviral.2003.07.004.

Atwell, J.E., Geoghegan, S., Karron, R.A., Polack, F.P., 2016. Clinical predictors of critical lower respiratory tract illness due to respiratory syncytial virus in infants and children: data to inform case definitions for efficacy trials. J. Infect. Dis. 214 (11), 1712–1716. https://doi.org/10.1093/infdis/jiw447.

Baccam, P., Beauchemin, C., Macken, C.A., Hayden, F.G., Perelson, A.S., 2006. Kinetics of influenza A virus infection in humans. J. Virol. 80 (15), 7590–7599. https://doi.org/10.1128/JVI.01623-05.

Bagga, B., Woods, C.W., Veldman, T.H., Gilbert, A., Mann, A., Balaratnam, G., Lambkin-Williams, R., Oxford, J.S., McClain, M.T., Wilkinson, T., Nicholson, B.P., Ginsburg, G.S., DeVincenzo, J.P., 2013. Comparing influenza and RSV viral disease dynamics in experimentally infected adults predicts clinical effectiveness of RSV antivirals. Antivir. Ther. 18, 785–791. https://doi.org/10.3851/IMP2629.

Beggs, N.F., Dobrovolny, H.M., 2015. Determining drug efficacy parameters for

mathematical models of influenza. J. Biol. Dyn. 9 (S1), 332–346. https://doi.org/10.1080/17513758.2015.1052764.
Bem, R.A., Domachowske, J.B., Rosenberg, H.F., 2011. Animal models of human respiratory syncytial virus disease. Am. J. Physiol. 301 (2), L148–L156. https://doi.org/10.1152/ajplung.00065.2011.
Bermejo-Martin, J.F., Tenorio, A., de Lejarazu, R.O., Eiros, J.M., Matias, V., Dominguez-Gil, M., Pino, M., Alonso, A., Blanco-Quiros, A., Arranz, E., Ardura, J., 2008. Similar cytokine profiles in response to infection with respiratory syncytial virus type A and type B in the upper respiratory tract in infants. Intervirology 51 (2), 112–115. https://doi.org/10.1159/000134268.
Bermingham, A., Collins, P.L., 1999. The M2-2 protein of human respiratory syncytial virus is a regulatory factor involved in the balance between RNA replication and transcription. Proc. Natl. Acad. Sci. USA 99, 11259–11264.
Blaschke, A.J., Allison, M.A., Meyers, L., Rogatcheva, M., Heyrend, C., Mallin, B., Carter, M., LaFleur, B., Barney, T., Poritz, M.A., Daly, J.A., Byington, C.L., 2011. Non-invasive sample collection for respiratory virus testing by multiplex PCR. J. Clin. Virol. 52 (3), 210–214. https://doi.org/10.1016/j.jcv.2011.07.015.
Bond, S., Draffan, A.G., Fenner, J.E., Lambert, J., Lim, C.Y., Lin, B., Luttick, A., Mitchell, J.P., Morton, C.J., Nearn, R.H., Sanford, V., Stanislawski, P.C., Tucker, S.P., 2015. The discovery of 1,2,3,9b-tetrahydro-5H-imidazo[2,1-a]isoindol-5-ones as a new class of respiratory syncytial virus (RSV) fusion inhibitors. Bioorg. Med. Chem. Lett. 25 (4), 969–975. https://doi.org/10.1016/j.bmcl.2014.11.018.
Bonfanti, J.-F., Meyer, C., Doublet, F., Fortin, J., Muller, P., Queguiner, L., Gevers, T., Janssens, P., Szel, H., Willebrords, R., Timmerman, P., Wuyts, K., van Remoortere, P., Janssens, F., Wigerinck, P., Andries, K., 2008. Selection of a respiratory syncytial virus fusion inhibitor clinical candidate. 2. discovery of a morpholinopropylaminobenzimidazole derivative (TMC353121). J. Med. Chem. 51 (4), 875–896. https://doi.org/10.1021/jm701284j.
Borchers, A.T., Chang, C., Gershwin, M.E., Gershwin, L.J., 2013. Respiratory syncytial virus – A comprehensive review. Clin. Rev. Allergy Immunol. 45 (3), 331–379. https://doi.org/10.1007/s12016-013-8368-9.
Brock, S.C., Goldenring, J.R., James, J., Crowe, E., 2003. Apical recycling systems regulate directional budding of respiratory syncytial virus from polarized epithelial cells. Proc. Natl. Acad. Sci. USA 100 (25), 15143–15148 (doi:10.1073pnas.2434327100).
Buckingham, S., Bush, A., Devincenzo, J., 2000. Nasal quantity of respiratory syncytial virus correlates with disease severity in hospitalized infants. Pediatr. Infect. Dis. J. 19 (2), 113–117. https://doi.org/10.1097/00006454-200002000-00006.
Capik, S.F., White, B.J., Lubbers, B.V., Apley, M.D., DeDonder, K.D., Larson, R.L., Harhay, G.P., Chitko-McKown, C.G., Harhay, D.M., Kalbfleisch, T.S., Schuller, G., Clawson, M.L., 2017. Comparison of the diagnostic performance of bacterial culture of nasopharyngeal swab and bronchoalveolar lavage fluid samples obtained from calves with bovine respiratory disease. Am. J. Veter-. Res. 78 (3), 350–358.
Chowdhury, M., Koyangi, Y., Suzuki, M., Kobayashi, S., Yamaguchi, K., Yamamoto, N., 1992. Increased production of human immunodeficiency virus (HIV) in HIV-induced syncytia formation – an efficient infection process. Virus Genes 6 (1), 63–78.
Chung, H.L., Park, H.J., Kim, S.Y., Kim, S.G., 2007. Age-related difference in immune responses to respiratory syncytial virus infection in young children. Pediatr. Allergy Immunol. 18 (2), 94–99. https://doi.org/10.1111/j.1399-3038.2006.00501.x.
Cianci, C., Meanwell, N., Krystal, M., 2005. Antiviral activity and molecular mechanism of an orally active respiratory syncytial virus fusion inhibitor. J. Antimicrob. Chemother. 55 (3), 289–292. https://doi.org/10.1093/jac/dkh558.
Coleman, T.F., Li, Y., 1996. An interior trust region approach for nonlinear minimization subject to bounds. SIAM J. Optim. 6 (2), 418–445.
Collins, P.L., Melero, J.A., 2011. Progress in understanding and controlling respiratory syncytial virus: still crazy after all these years. Virus Res. 162 (1–2), 80–99. https://doi.org/10.1016/j.virusres.2011.09.020.
Conn, A., Gould, N., Toint, P., 1997. A globally convergent lagrangian barrier algorithm for optimization with general inequality constraints and simple bounds. Math. Comput. Am. Math. Soc. 66 (217), 261–288.
Davis, M.M., Butchart, A.T., Wheeler, J.R., Coleman, M.S., Singer, D.C., Freed, G.L., 2011. Failure-to-success ratios, transition probabilities and phase lengths for prophylactic vaccines versus other pharmaceuticals in the development pipeline. Vaccine 29 (5), 9414–9416. https://doi.org/10.1016/j.vaccine.2011.09.128.
Dayar, G.T., Kocabas, E., 2016. Respiratory syncytial virus infections. J. Pediatr. Inf. 10 (2), 60–67. https://doi.org/10.5152/ced.2016.2238.
DeVincenzo, J.P., Wilkinson, T., Vaishnaw, A., Cehelsky, J., Myers, R., Nochur, S., Harrison, L., Meeking, P., Mann, A., Moane, E., Oxford, J., Pareek, R., Moore, R., Walsh, E., Studholme, R., Dorsett, P., Alvarez, R., Lambkin-Williams, R., 2010. Viral load drives disease in humans experimentally infected with respiratory syncytial virus. Am. J. Respir. Crit. Care Med. 182, 1305–1314. https://doi.org/10.1164/rccm.201002–02210 C.
DeVincenzo, J., Lambkin-Williams, R., Wilkinson, T., Cehelsky, J., Nochur, S., Walsh, E., Meyers, R., Gollob, J., Vaishnaw, A., 2010. A randomized, double-blind, placebo-controlled study of an RNAi-based therapy directed against respiratory syncytial virus. Proc. Natl. Acad. Sci. USA 107 (19), 8800–8805. https://doi.org/10.1073/pnas.0912186107.
DeVincenzo, J.P., McClure, M.W., Symons, J.A., Fathi, H., Westland, C., Chanda, S., Lambkin-Williams, R., Smith, P., Zhang, Q., Beigelman, L., Blatt, L.M., Fry, J., 2015. Activity of oral ALS-008176 in a respiratory syncytial virus challenge study. N. Engl. J. Med. 373 (21), 2048–2058F. https://doi.org/10.1056/NEJMoa1413275.
DeVincenzo, J., 2004. Natural infection of infants with respiratory syncytial virus subgroups A and B: a study of frequency, disease severity, and viral load. Pediatr. Res. 56 (6), 914–917. https://doi.org/10.1203/01.PDR.0000145255.86117.6A.
Dunne, J., Rodriguez, W.J., Murphy, D., Beasley, B.N., Burckart, G.J., Filie, J.D., Lewis, L.L., Sachs, H.C., Sheridan, P.H., Starke, P., Yao, L.P., 2011. Extrapolation of adult data and other data in pediatric drug-development programs. Ped 128 (5), E1242–E1249. https://doi.org/10.1542/peds.2010-3487.
Eckardt-Michel, J., Lorek, M., Baxmann, D., Grunwald, T., Keil, G.M., Zimmer, G., 2008. The fusion protein of respiratory syncytial virus triggers p53-dependent apoptosis. J. Virol. 82 (7), 3236–3249. https://doi.org/10.1128/JVI.01887-07.
Esposito, S., Pietro, G.Di, 2016. Respiratory syncytial virus vaccines: an update on those in the immediate pipeline. Future Microbiol. 11 (11), 1479–1490. https://doi.org/10.2217/fmb-2016-0106.
Falsey, A.R., Walsh, E.E., 2005. Respiratory syncytial virus infection in elderly adults. Drugs Aging 22 (7), 577–587.
Fang, J., Jadhav, P.R., 2012. From in vitro EC_{50} to in vivo dose-response for anti-retrovirals using an HIV disease model. part I: a framework. Clin. Microbiol. Rev. 39 (4), 357–368. https://doi.org/10.1007/s10928-012-9255-3.
Feldman, S., Audet, S., Beeler, J., 2000. The fusion glycoprotein of human respiratory syncytial virus facilitates virus attachment and infectivity via an interaction with cellular heparan sulfate. J. Virol. 74 (14), 6442–6447. https://doi.org/10.1128/JVI.74.14.6442-6447.2000.
Feng, S., Hong, D., Wang, B., Zheng, X., Miao, K., Wang, L., Yun, H., Gao, L., Zhao, S., Shen, H.C., 2015. Discovery of imidazopyridine derivatives as highly potent respiratory syncytial virus fusion inhibitors. ACS Med. Chem. Lett. 6 (3), 359–362. https://doi.org/10.1021/acsmedchemlett.5b00008.
Ferguson, N., Fraser, C., Anderson, R., 2001. Viral dynamics and anti-viral pharmacodynamics: rethinking in vitro measures of drug potency. Trends Pharmacol. Sci. 22 (2), 97–100. https://doi.org/10.1016/S0165-6147(00)01615-1.
Foerster, A., Maertens, G.N., Farrell, P.J., Bajorek, M., 2015. Dimerization of matrix protein is required for budding of respiratory syncytial virus. J. Virol. 89 (8), 4624–4635. https://doi.org/10.1128/JVI.03500-14.
Follett, E., Pringle, C., Pennington, T., 1975. Virus development in enucleate cells – echovirus, poliovirus, pseudorabies virus, reovirus, respiratory syncytial virus and semliki forest virus. J. Gen. Virol. 26, 183–196. https://doi.org/10.1099/0022-1317-26-2-183.
Gilca, R., De Serres, G., Tremblay, M., Vachon, M., Leblanc, E., Bergeron, M., Dery, P., Boivin, G., 2006. Distribution and clinical impact of human respiratory syncytial virus genotypes in hospitalized children over 2 winter seasons. J. Infect. Dis. 193 (1), 54–58. https://doi.org/10.1086/498526.
Golberg, D.E., 1989. Genetic algorithms in search, optimization, and machine learning. Addion wesley.
González-Parra, G., Dobrovolny, H.M., 2018. Modeling of fusion inhibitor treatment of RSV in African green monkeys. J. Theor. Biol. https://doi.org/10.1016/j.jtbi.2018.07.02.
González-Parra, G., Dobrovolny, H.M., 2015. Assessing uncertainty in A2 respiratory syncytial virus viral dynamics. Comput. Math. Meth. Med 2015, 567589. https://doi.org/10.1155/2015/567589.
González-Parra, G., Dobrovolny, H.M., Aranda, D.F., Chen-Charpentier, B., Roja, R.A.G. Quantifying rotavirus kinetics in the REH tumor cell line using in vitro data. Virus Res.
González-Parra, G., Rodriguez, T., Dobrovolny, H.M., 2016. A comparison of methods for extracting influenza viral titer characteristics. J. Virol. Methods 231, 14–24. https://doi.org/10.1016/j.jviromet.2016.02.005.
González-Parra, G., De Ridder, F., Huntjens, D., Roymans, D., Ispas, G., Dobrovolny, H.M., 2018. A comparison of RSV and influenza in vitro kinetic parameters reveals differences in infecting time. Plos One 13 (2), e0192645. https://doi.org/10.1371/journal.pone.0192645.
Gonzalez-Reyes, L., Ruiz-Arguello, M., Garcia-Barreno, B., Calder, L., Lopez, J., Albar, J., Skehel, J., Wiley, D., Melero, J., 2001. Cleavage of the human respiratory syncytial virus fusion protein at two distinct sites is required for activation of membrane fusion. Proc. Natl. Acad. Sci. USA 98 (17), 9859–9864. https://doi.org/10.1073/pnas.151098198.
Groskreutz, D.J., Monick, M.M., Yarovinsky, T.O., Powers, L.S., Quelle, D.E., Varga, S.M., Look, D.C., Hunninghake, G.W., 2007. Respiratory syncytial virus decreases p53 protein to prolong survival of airway epithelial cells. J. Immunol. 179 (5), 2741–2747.
Hall, C., Walsh, E., Schnabel, K., Long, C., McConnochie, K., Hildreth, S., Anderson, L., 1990. Occurrence of group A and group B of respiratory syncytial virus over 15 years – associated epidemiologic and clinical characteristics in hospitalized and ambulatory children. J. Infect. Dis. 162 (6), 1283–1290. https://doi.org/10.1093/infdis/162.6.1283.
Hall, C., Walsh, E., Long, C., Schnabel, K., 1991. Immunity to and frequency of reinfection with respiratory syncytial virus. J. Infect. Dis. 163 (4), 693–698.
Hall, C., Long, C., Schnabel, K., 2001. Respiratory syncytial virus infections in previously healthy working adults. Clin. Inf. Dis. 33 (6), 792–796. https://doi.org/10.1086/322657.
Hendry, R., Talis, A., Godfrey, E., Anderson, L., Fernie, B., McIntosh, K., 1986. Concurrent circulation of antigenically distinct strains of respiratory syncytial virus during community outbreaks. J. Infect. Dis. 153 (2), 291–297. https://doi.org/10.1093/infdis/153.2.291.
Holder, B.P., Beauchemin, C.A., 2011. Exploring the effect of biological delays in kinetic models of influenza within a host or cell culture. BMC Public Health 11 (S1), S10. https://doi.org/10.1186/1471-2458-11-S1-S10.
Holford, N., Sheiner, L., 1981. Understanding the dose-effect relationship: clinical application of pharmacokinetic-pharmacodynamic models. Clin. Pharmacokinet. 6 (6), 429–453.
Holland, J.H., 1992. Genetic algorithms. Sci. Am. 267 (1), 66–72.
Hornsleth, A., Klug, B., Nir, M., Johansen, J., Hansen, K., Christensen, L., Larsen, L., 1998. Severity of respiratory syncytial virus disease related to type and genotype of virus and to cytokine values in nasopharyngeal secretions. Pediatr. Infect. Dis. J. 17 (12), 1114–1121. https://doi.org/10.1097/00006454-199812000-00003.

Houben, M., Coenjaerts, F., Rossen, J., Belderbos, M., Hofland, R., Kimpen, J., Bont, L., 2010. Disease severity and viral load are correlated in infants with primary respiratory syncytial virus infection in the community. J. Med. Virol. 82 (7), 1266–1271. https://doi.org/10.1002/jmv.21771.

Ispas, G., Koul, A., Verbeeck, J., Sheehan, J., Sanders-Beer, B., Roymans, D., Andries, K., Rouan, M.-C., De Jonghe, S., Bonfanti, J.-F., Vanstockem, M., Simmen, K., Verloes, R., 2015. Antiviral activity of TMC353121, a respiratory syncytial virus (RSV) fusion inhibitor, in a non-human primate model. PLOS One 10 (5), e0126959. https://doi.org/10.1371/journal.pone.0126959.

Jafri, H.S., Wu, X., Makari, D., Henrickson, K.J., 2013. Distribution of respiratory syncytial virus subtypes A and B among infants presenting to the emergency department with lower respiratory tract infection or apnea. Pediatr. Infect. Dis. J. 32 (4), 335–340. https://doi.org/10.1097/INF.0b013e318282603a.

Jia, N., Barclay, W.S., Roberts, K., Yen, H.-L., Chan, R.W., Lam, A.K., Air, G., Peiris, J.M., Dell, A., Nicholls, J.M., Haslam, S.M., 2014. Glycomic characterization of respiratory tract tissues of ferrets implications for its use in influenza virus infection studies. J. Biol. Chem. 289 (41), 28489–28504. https://doi.org/10.1074/jbc.M114.588541.

Jones, B.G., Sealy, R.E., Rudraraju, R., Traina-Dorge, V.L., Finneyfrock, B., Cook, A., Takimoto, T., Portner, A., Hurwitz, J.L., 2012. Sendai virus-based RSV vaccine protects african green monkeys from RSV infection. Vaccine 30 (48). https://doi.org/10.1016/j.vaccine.2012.09.038. (6955–6955).

Jorquera, P.A., Anderson, L., Tripp, R.A., 2016. Understanding respiratory syncytial virus (RSV) vaccine development and aspects of disease pathogenesis. Expert Rev. Vaccin. 15 (2), 173–187. https://doi.org/10.1586/14760584.2016.1115353.

Kakuk, T., Soike, K., Brideau, R., Zaya, R., Cole, S., Zhang, J., Roberts, E., Wells, P., Wathen, M., 1993. A humand respiratory syncytial virus (RSV) primate model of enhanced pulmonary pathology induced with a formalin-inactivated RSV vaccine but not a recombinant FG subunit vaccine. J. Infect. Dis. 167 (3), 553–561.

Kaneko, M., Watanabe, J., Ueno, E., Hida, M., Sone, T., 2001. Risk factors for severe respiratory syncytial virus-associated lower respiratory tract infection in children. Pediatr. Int. 43 (5), 489–492. https://doi.org/10.1046/j.1442-200X.2001.01438.x.

Kulkarni, H., Smith, C.M., Lee, D.D.H., Hirst, R.A., Easton, A.J., O'Callaghan, C., 2016. Evidence of respiratory syncytial virus spread by aerosol time to revisit infection control strategies? Am. J. Resp. Crit. Care Med. 194 (3), 308–316. https://doi.org/10.1164/rccm.201509-1833OC.

Lee, F.E.-H., Walsh, E.E., Falsey, A.R., Betts, R.F., Treanor, J.J., 2004. Experimental infection of humans with A2 respiratory syncytial virus. Antivir. Res. 63, 191–196. https://doi.org/10.1016/j.antiviral.2004.04.005.

Lee, W.-J., Kim, Y.-J., Kim, D.-W., Lee, H.S., Lee, H.Y., Kim, K., 2012. Complete genome sequence of human respiratory syncytial virus genotype A with a 72-nucleotide duplication in the attachment protein G gene. J. Virol. 86 (24), 13810–13811. https://doi.org/10.1128/JVI.02571-12.

Levitz, R., Wattier, R., Phillips, P., Solomon, A., Lawler, J., Lazar, I., Weibel, C., Kahn, J.S., 2012. Induction of IL-6 and CCL5 (RANTES) in human respiratory epithelial (A549) cells by clinical isolates of respiratory syncytial virus is strain specific. Virol. J. 9, 190. https://doi.org/10.1186/1743-422X-9-190.

Levitz, R., Gao, Y., Dozmorov, I., Song, R., Wakeland, E.K., Kahn, J.S., 2017. Distinct patterns of innate immune activation by clinical isolates of respiratory syncytial virus. PLoS One 12 (9), e0184318. https://doi.org/10.1371/journal.pone.0184318.

Liesman, R.M., Buchholz, U.J., Luongo, C.L., Yang, L., Proia, A.D., DeVincenzo, J.P., Collins, P.L., Pickles, R.J., 2014. RSV-encoded NS2 promotes epithelial cell shedding and distal airway obstruction. J. Clin. Investig. 124 (5), 2219–2233. https://doi.org/10.1172/JCI72948.

Lukacs, N.W., Moore, M.L., Rudd, B.D., Berlin, A.A., Collins, R.D., Olson, S.J., Ho, S.B., Stokes Peebles, J.R., 2006. Differential immune responses and pulmonary pathophysiology are induced by two different strains of respiratory syncytial virus. Am. J. Pathol. 169 (3), 977–986. https://doi.org/10.2353/ajpath.2006.051055.

Lundin, A., Bergstrom, T., Bendrioua, L., Kann, N., Adamiak, B., Trybala, E., 2010. Two novel fusion inhibitors of human respiratory syncytial virus. Antivir. Res. 88 (3), 317–324. https://doi.org/10.1016/j.antiviral.2010.10.004.

Malloy, A.M., Falsey, A.R., Ruckwardt, T.J., 2013. Consequences of Immature and Senescent Immune Responses for Infection with Respiratory Syncytial Virus. Curr. Top. Microbiol. Immunol. 372, 211–231. https://doi.org/10.1007/978-3-642-38919-1_11.

Marquez, A., Hsiung, G., 1967. Influence of glutamine on multiplication and cytopathic effect of respiratory syncytial virus. Proc. Soc. Exp. Biol. Med. 124, 95–99.

Mcintosh, K., Masters, H., Orr, I., Chao, R., Barkin, R., 1978. Immunological response to infection with respiratory syncytial virus in infants. J. Infect. Dis. 138 (1), 24–32.

McIntosh, E., Desilva, L., Oates, R., 1993. Clinical severity of respiratory syncytial virus group A and group B infection in Sydney, Australia. Pediatr. Infect. Dis. J. 12 (10), 815–819.

Meerhoff, T., Houben, M., Coenjaerts, F., Kimpen, J., Hofland, R., Schellevis, F., Bont, L., 2010. Detection of multiple respiratory pathogens during primary respiratory infection: nasal swab versus nasopharyngeal aspirate using real-time polymerase chain reaction. Eur. J. Clin. Microbiol. Infect. Dis. 29 (4), 365–371. https://doi.org/10.1007/s10096-009-0865-7.

Miao, H., Xia, X., Perelson, A.S., Wu, H., 2011. On identifiability of nonlinear ODE models and applications in viral dynamics. SIAM Rev. 53 (1), 3–39. https://doi.org/10.1137/090757009.

Mills, J., Vankirk, J., Wright, P., Chanock, R., 1971. Experimental respiratory syncytial virus infection of adults – possible mechanisms of resistance to infection and illness. J. Immunol. 107 (1), 123–130.

Mistry, B.A., D'Orsogna, M.R., Chou, T., 2018. The effects of statistical multiplicity of infection on virus quantification and infectivity assays. Biophys. J. 114 (12), 2974–2985. https://doi.org/10.1016/j.bpj.2018.05.005.

Mosquera, R.A., Stark, J.M., Atkins, C.L., Colasurdo, G.N., Chevalier, J., Samuels, C.L., Pacheco, S.S., 2014. Functional and immune response to respiratory syncytial virus infection in aged BALB/c mice: a search for genes determining disease severity. Exp. Lung Res. 40 (1), 40–49. https://doi.org/10.3109/01902148.2013.859334.

Mulugeta, Y., Barrett, J.S., Nelson, R., Eshete, A.T., Mushtaq, A., Yao, L., Glasgow, N., Mulberg, A.E., Gonzalez, D., Green, D., Florian, J., Krudys, K., Seo, S., Kim, I., Chilukuri, D., Burckart, G.J., 2016. Exposure matching for extrapolation of efficacy in pediatric drug development. J. Clin. Pharmacol. 56 (11), 1326–1334. https://doi.org/10.1002/jcph.744.

Naorat, S., Chittaganpitch, M., Thamthitiwat, S., Henchaichon, S., Sawatwong, P., Srisaengchai, P., Lu, Y., Chuananon, S., Amornintapichet, T., Chantra, S., Erdman, D.D., Maloney, S.A., Akarasewi, P., Baggett, H.C., 2013. Hospitalizations for acute lower respiratory tract infection due to respiratory syncytial virus in thailand, 2008–2011. J. Infect. Dis. 203 (S3), S238–S245. https://doi.org/10.1093/infdis/jit456.

Neumann, A.U., Lam, N.P., Dahari, H., Gretch, D.R., Wiley, T.E., Layden, T.J., Perelson, A.S., 1998. Hepatitis C viral dynamics in vivo and the antiviral efficacy of interferon-α therapy. Science 282, 103–107.

Nguyen, T.D., Thi, M.H.P., Ha, M.T., Thi, T.L.T., Thi, K.H.D., Yoshida, L.-M., Okitsu, S., Hayakawa, S., Mizuguchi, M., Ushijima, H., 2013. Molecular epidemiology and disease severity of human respiratory syncytial virus in Vietnam. PLoS One 8 (1), e45436. https://doi.org/10.1371/journal.pone.0045436.

Nguyen, V.K., Binder, S.C., Boianelli, A., Meyer-Hermann, M., Hernandez-Vargas, E.A., 2015. Ebola virus infection modeling and identifiability problems. Front. Microbiol. 6, 257. https://doi.org/10.3389/fmicb.2015.00257.

Openshaw, P.J., Chiu, C., Culley, F.J., Johansson, C., 2017. Prot. Harmful Immun. RSV Infect. 35, 501–532. https://doi.org/10.1146/annurev-immunol-051116-052206.

Papadopoulos, N., Gourgiotis, D., Javadyan, A., Bossios, A., Kallergi, K., Psarras, S., Tsolia, M., Kafetzis, D., 2004. Does respiratory syncytial virus subtype influences the severity of acute bronchiolitis in hospitalized infants? Resp. Med. 98 (9), 879–882. https://doi.org/10.1016/j.rmed.2004.01.009.

Paradis, E.G., Pinilla, L.T., Holder, B.P., Abed, Y., Boivin, G., Beauchemin, C.A.A., 2015. Impact of the H275Y and I223V mutations in the neuraminidase of the 2009 pandemic influenza virus in vitro and evaluating experimental reproducibility. PLOS One 10 (5), e0126115. https://doi.org/10.1371/journal.pone.0126115.

Park, S.Y., Kim, T., Jang, Y.R., Kim, M.-C., Chong, Y.P., Lee, S.-O., Choi, S.-H., Kim, Y.S., Woo, J.H., Kim, S.-H., 2016. Factors predicting life-threatening infections with respiratory syncytial virus in adult patients. Infect. Dis. 1–8.

Perelson, A.S., Neumann, A., Markowitz, M., Leonard, J., Ho, D., 1996. HIV-1 dynamics in vivo: virion clearance rate, infected cell life-span, and viral generation time. Science 271 (5255), 1582–1586.

Perron, M., Stray, K., Kinkade, A., Theodore, D., Lee, G., Eisenberg, E., Sangi, M., Gilbert, B.E., Jordan, R., Piedra, P.A., Toms, G.L., Mackman, R., Cihlar, T., 2016. GS-5806 inhibits a broad range of respiratory syncytial virus clinical isolates by blocking the virus-cell fusion process. Antimicrob. Agents Chemother. 60 (3), 1264–1273. https://doi.org/10.1128/AAC.01497-15.

Petrie, S.M., Butler, J., Barr, I.G., McVernon, J., Hurt, A.C., McCaw, J.M., 2015. Quantifying relative within-host replication fitness in influenza virus competition experiments. J. Theor. Biol. 382, 259–271. https://doi.org/10.1016/j.jtbi.2015.07.003.

Pinilla, L.T., Holder, B.P., Abed, Y., Boivin, G., Beauchemin, C.A.A., 2012. The H275Y neuraminidase mutation of the pandemic A/H1N1 influenza virus lengthens the eclipse phase and reduces viral output of infected cells, potentially compromising fitness in ferrets. J. Virol. 86 (19), 10651–10660. https://doi.org/10.1128/JVI.07244-11.

Press, W.H., Teukolsky, S.A., Vetterling, W.T., Flannery, B.P., 1992. Numerical recipes: The art of scientific computing (cambridge).

Rodriguez-Fernandez, R., Tapia, L.I., Yang, C.-F., Torres, J.P., Chavez-Bueno, S., Garcia, C., Jaramillo, L.M., Moore-Clingenpeel, M., Jafri, H.S., Peeples, M.E., Piedra, P.A., Ramilo, O., Mejias, A., 2018. Respiratory syncytial virus genotypes, host immune profiles, and disease severity in young children hospitalized with bronchiolitis. J. Infect. Dis. 217 (1), 24–34. https://doi.org/10.1093/infdis/jix543.

Ruckwardt, T.J., Morabito, K.M., Graham, B.S., 2016. Determinants of early life immune responses to RSV infection. Curr. Opin. Virol. 16, 151–157. https://doi.org/10.1016/j.coviro.2016.01.003.

Russell, C.D., Unger, S.A., Walton, M., Schwarze, J., 2017. The human immune response to respiratory syncytial virus infection. Clin. Microbiol. Rev. 30 (2), 481–502. https://doi.org/10.1128/CMR.00090-16.

Russi, J., Chiparelli, H., Montano, A., Etorena, P., Hortal, M., 1989. Respiratory syncytial virus subgroups and pneumonia in children. Lancet 2 (8670), 1039–1040.

Rutigliano, J., Johnson, T., Hollinger, T., Fischer, J., Aung, S., Graham, B., 2004. Treatment with anti-LFA-1 delays the CD8(+) cytotoxic-T-lymphocyte response and viral clearance in mice with primary respiratory syncytial virus infection. J. Virol. 78 (6), 3014–3023. https://doi.org/10.1128/JVI.78.6.3014-3023.2004.

Sacco, R.E., Durbin, R.K., Durbin, J.E., 2015. Animal models of respiratory syncytial virus infection and disease. Curr. Opin. Virol. 13, 117–122. https://doi.org/10.1016/j.coviro.2015.06.003.

Sarmiento, R.E., Tirado, R.G., Valverde, L.E., Gomez-Garcia, B., 2007. Kinetics of antibody-induced modulation of respiratory syncytial virus antigens in a human epithelial cell line. Virol. J. 4, 68. https://doi.org/10.1186/1743-422X-4-68.

Shahrabadi, M.S., Lee, P.W.K., 1988. Calcium requirement for syncytium formation in HEp-2 cells by respiratory syncytial virus. J. Clin. Microbiol. 26 (1) (139–131).

Shahriari, S., Gordon, J., Ghildyal, R., 2016. Host cytoskeleton in respiratory syncytial virus assembly and budding. Virol. J. 13, 161. https://doi.org/10.1186/s12985-016-0618-z.

Shaikh, F.Y., Utley, T.J., Craven, R.E., Rogers, M.C., Lapierre, L.A., Goldenring, J.R., James, J., Crowe, E., 2012. Respiratory syncytial virus assembles into structured

filamentous virion particles independently of host cytoskeleton and related proteins. PLoS One 7 (7), e40826. https://doi.org/10.1371/journal.pone.0040826.
Shakeri, A., Mastrangelo, P., Griffin, J.K., Moraes, T.J., Hegele, R.G., 2015. Respiratory syncytial virus receptor expression in the mouse and viral tropism. Histol. Histopathol. 30 (4), 401–411.
Shi, T., Balsells, E., Wastnedge, E., Singleton, R., Rasmussen, Z., Zar, H.J., Rath, B.A., Madhi, S.A., Campbell, S., Vaccari, L.C., Bulkow, L.R., Thomas, E.D., Barnett, W., Hoppe, C., Campbell, H., Nair, H., 2015. Risk factors for respiratory syncytial virus associated with acute lower respiratory infection in children under five years: systematic review and meta-analysis. J. Glob. Health 5 (2), 203–215. https://doi.org/10.7189/jogh.05.020416.
Shigeta, S., Hinuma, Y., Suto, T., Ishida, N., 1968. Cell to cell infection of respiratory syncytial virus in Hep-2 monolayer cultures. J. Gen. Virol. 3 (1), 129–131. https://doi.org/10.1099/0022-1317-3-1-129.
Simon, P.F., de La Vega, M.-A., Paradis, É., Mendoza, E., Coombs, K.M., Kobasa, D., Beauchemin, C.A.A., 2016. Avian influenza viruses that cause highly virulent infections in humans exhibit distinct replicative properties in contrast to human H1N1 viruses. Sci. Rep. 6, 24154. https://doi.org/10.1038/srep24154.
Stein, R.T., Bont, L.J., Zar, H., Polack, F.P., Park, C., Claxton, A., Borok, G., Butylkova, Y., Wegzyn, C. Respiratory syncytial virus hospitalization and mortality: Systematic review and meta-analysis. Pediatr. Pulmonol. http://dx.doi.org/10.1002/ppul.23570.
Stokes, K.L., Chi, M.H., Sakamoto, K., Newcomb, D.C., Currier, M.G., Huckabee, M.M., Lee, S., Goleniewska, K., Pretto, C., Williams, J.V., Hotard, A., Sherrill, T.P., Stokes Peebles, J.R., Moore, M.L., 2011. Differential pathogenesis of respiratory syncytial virus clinical isolates in BALB/c mice. J. Virol. 85 (12), 5782–5793. https://doi.org/10.1128/JVI.01693-10.
Straub, C.P., Lau, W.-H., Preston, F.M., Headlam, M.J., Gorman, J.J., Collins, P.L., Spann, K.M., 2011. Mutation of the elongin C binding domain of human respiratory syncytial virus non-structural protein 1 (NS1) results in degradation of NS1 and attenuation of the virus. Virol. J. 8, 252. https://doi.org/10.1186/1743-422X-8-252.
Sun, Z., Pan, Y., Jiang, S., Lu, L., 2013. Respiratory syncytial virus entry inhibitors targeting the F protein. Viruses—Basel 5 (1), 211–225. https://doi.org/10.3390/v5010211.
Sylwester, A., Murphy, S., Shutt, D., Soll, D., 1997. HIV-induced T cell syncytia are self-perpetuating and the primary cause of T cell death in culture. J. Immunol. 158 (8), 3996–4007.
Symeonides, M., Murooka, T.T., Bellfy, L.N., Roy, N.H., Mempel, T.R., Thali, M., 2015. HIV-1-induced small T cell syncytia can transfer virus particles to target cells through transient contacts. Viruses—Basel 7 (12), 6590–6603. https://doi.org/10.3390/v7122959.
Taylor, G., 2017. Animal models of respiratory syncytial virus infection. Vaccine 35 (3), 469–480. https://doi.org/10.1128/JVI.00384-06.
Teng, M., Whitehead, S., Collins, P., 2001. Contribution of the respiratory syncytial virus G glycoprotein and its secreted and membrane-bound forms to virus replication in vitro and in vivo. Virol 289 (2), 283–296. https://doi.org/10.1006/viro.2001.1138.
Tregoning, J.S., Schwarze, J., 2010. Respiratory viral infections in infants: causes, clinical symptoms, virology, and immunology. Clin. Microbiol. Rev. 23 (1), 74–98. https://doi.org/10.1128/CMR.00032-09.
Vanover, D., Smith, D.V., Blanchard, E.L., Alonas, E., Kirschman, J.L., Lifland, A.W., Zurla, C., Santangelo, P.J., 2017. RSV glycoprotein and genomic RNA dynamics reveal filament assembly prior to the plasma membrane. Nat. Comm. 8, 667. https://doi.org/10.1038/s41467-017-00732-z.
Villenave, R., O'Donoghue, D., Thavagnanam, S., Touzelet, O., Skibinski, G., Heaney, L.G., McKaigue, J.P., Coyle, P.V., Shields, M.D., Power, U.F., 2011. Differential cytopathogenesis of respiratory syncytial virus prototypic and clinical isolates in primary pediatric bronchial epithelial cells. Virol. J. 8, 43. https://doi.org/10.1186/1743-422X-8-43.
Villenave, R., Thavagnanam, S., Sarlang, S., Parker, J., Douglas, I., Skibinski, G., Heaney, L.G., McKaigue, J.P., Coyle, P.V., Shields, M.D., Power, U.F., 2012. In vitro modeling of respiratory syncytial virus infection of pediatric bronchial epithelium, the primary target of infection in vivo. Proc. Natl. Acad. Sci. USA 109 (13), 5040–5045. https://doi.org/10.1073/pnas.1110203109.
Walsh, E.E., Peterson, D.R., Falsey, A.R., 2013. Viral shedding and immune responses to respiratory syncytial virus infection in older adults. J. Infect. Dis. 207, 1424–1432. https://doi.org/10.1093/infdis/jit038.
Weiss, K.A., Knudson, C.J., Christiaansen, A.F., Varga, S.M., 2014. Animal models of human respiratory viral infections. In: Singh, S. (Ed.), Human Respiratory Viral Infections, CRC Press, Boca Raton, FL, USA, pp. 129–161.
Yui, I., Hoshi, A., Shigeta, Y., Takami, T., Nakayama, T., 2003. Detection of human respiratory syncytial virus sequences in peripheral blood mononuclear cells. J. Med. Virol. 70 (3), 481–489. https://doi.org/10.1002/jmv.10421.
Zanin, M., Baviskar, P., Webster, R., Webby, R., 2016. The interaction between respiratory pathogens and mucus. Cell Host Microbe 19 (2), 159–168. https://doi.org/10.1016/j.chom.2016.01.001.
Zheng, X., Wang, L., Wang, B., Miao, K., Xiang, K., Feng, S., Gao, L., Shen, H.C., Yun, H., 2016. Discovery of piperazinylquinoline derivatives as novel respiratory syncytial virus fusion inhibitors. ACS Med. Chem. Lett. 7 (6), 558–562. https://doi.org/10.1021/acsmedchemlett.5b00234.